Published in final edited form as:
Ophthalmology. 2011 April ; 118(4): 679–686. doi:10.1016/j.ophtha.2010.08.018.

Progression of Geographic Atrophy in Age-Related Macular Degeneration Imaged with Spectral Domain Optical Coherence Tomography

Zohar Yehoshua, MD, MHA, **Philip J. Rosenfeld, MD PhD**, **Giovanni Gregori, PhD**, **William J. Feuer, MS**, **Manuel Falcão, MD**, **Brandon J. Lujan, MD**, and **Carmen Puliafito, MD, MBA**
Department of Ophthalmology, Bascom Palmer Eye Institute, University of Miami Miller School of Medicine, Miami, FL

Abstract

Purpose—To determine the area and enlargement rate (ER) of geographic atrophy (GA) in patients with age-related macular degeneration (AMD) using the spectral-domain optical coherence tomography (SDOCT) fundus image.

Design—Prospective longitudinal natural history study

Participants—Eighty-six eyes of 64 patients with at least 6 months follow-up.

Methods—Patients with GA secondary to AMD were enrolled in this study. Macular scans were performed using the Cirrus SDOCT (Carl Zeiss Meditec, Dublin CA). The areas of GA identified on the SDOCT fundus images were quantified using a digitizing tablet. Reproducibility of these measurements was assessed and the ER of GA was calculated. The usefulness of performing square root transformations of the lesion area measurements was explored.

Main Outcome Measure—Enlargement rate of GA

Results—At baseline, 27% of eyes had a single area of GA. The mean total area at baseline was 4.59mm^2 (1.8 disc areas (DA)). The mean follow up time was 1.24 years. Reproducibility, as assessed with the intraclass correlation coefficient (ICC), was excellent on both the original area scale (ICC = 0.995) and the square-root scale (ICC=0.996). Inter-grader differences were not an important source of variability in lesion size measurement (ICC=0.999, 0.997). On average, the ER of GA per year was 1.2 mm^2 (0.47 DA; range [0.01 - 3.61 mm^2/year]. The ER correlated with the initial area of GA (r=0.45, p<0.001), but there were variable growth rates for any given baseline area. When the square root transformation of the lesion area measurements was used as a measure of lesion size, the enlargement rate (0.28 mm/yr) was not correlated with baseline size

Corresponding author: Philip J. Rosenfeld, MD, PhD, Bascom Palmer Eye Institute, 900 NW 17th St., Miami, FL 33136. Telephone: 305-326-6148, Fax: 305-326-6417, prosenfeld@med.miami.edu.

Presented as a poster at the 2009 Association for Research in Vision and Ophthalmology Meeting in Fort Lauderdale, Florida and at the 2009 Combined Retinal Congress Meeting in New York City.

Financial disclosure: Drs. Yehoshua, Rosenfeld, Gregori, and Lujan received research support from Carl Zeiss Meditec, Inc. Giovanni Gregori and the University of Miami co-own a patent that is licensed to Carl Zeiss Meditec, Inc. Philip Rosenfeld has received honoraria for lectures from Carl Zeiss Meditec, Inc. Carmen Puliafito is a consultant for Carl Zeiss Meditec, Inc and co-owns a patent that is licensed to Carl Zeiss Meditec, Inc. William Feuer and Manuel Falcão have no financial or proprietary interest in the materials presented herein.

(r=-0.09,p=0.40). In this cohort of lesions, no correlation was found between ER and length of follow-up. Square root transformation of the data helped facilitate sample size estimates for controlled clinical trials involving GA.

Conclusions—The SDOCT fundus image can be used to visualize and quantify GA. Advantages of this approach include the convenience and assurance of using a single imaging technique that permits simultaneous visualization of GA along with the loss of photoreceptors and the retinal pigment epithelium which should correlate with the loss of visual function.

Keywords

geographic atrophy; age-related macular degeneration; optical coherence tomography; enlargement rate; progression

Introduction

Geographic atrophy (GA) is a significant cause of both moderate and severe central visual loss and is bilateral in most patients with advanced age-related macular degeneration (AMD).[1-4] GA represents the loss of photoreceptors, retinal pigment epithelium (RPE), and choriocapillaris within the macula. The natural history of GA has been described as a progressive condition that evolves through stages with loss of vision occurring over years.[3-5] In the United States, GA is present in 3.5% of people aged 75 years and older, and its prevalence rises to 22% or more in those older than 90 years.[6-8]

Quantifying the progression of GA with respect to area was first reported by Schatz and McDonald in 1989.[1] These authors evaluated fundus photographs of 50 eyes with GA from AMD and they reported an average enlargement rate (ER) of139 μm/year in the horizontal direction. In a retrospective population based study (Beaver Dam Eye Study), Klein et al. described the five year ER in total area and greatest linear dimension (GLD) in 53 eyes of 32 patients with GA.[9] The overall increase in atrophy was 6.4 mm^2 (2.5 disc areas [DA]) over a period of five years and all study eyes showed progression of GA. In a prospective natural history study of GA, Sunness et al. studied 212 eyes of 131 patients and found that the median overall ER was 2.1 mm^2/year (mean, 2.6 mm^2/year).[10] The Age-Related Eye Disease Study (AREDS) group reported a mean change in area of 7.45 mm^2 from baseline at 4 years and an overall ER of 1.78 mm^2 per year.[11] All these data were collected using color fundus photography to image GA. However, quantitating GA using color fundus photography can be challenging and the reproducibility of detecting and accurately delineating GA by fundus photography has been reported by several groups to be only moderate.[12-16]

Another strategy for imaging GA is fundus autofluorescence (FAF) using a confocal scanning laser ophthalmoscope (SLO) or a fundus camera. The assumption when using FAF to image GA is that the loss of autofluorescence in the posterior pole of AMD patients correlates with the loss of lipofuscin, the most prominent fluorophore in the posterior pole which is contained within the RPE. Thus, an area of decreased autofluorescence is an indirect assessment of the RPE integrity with absent autofluorescence thought to represent an area of absent RPE. In the Fundus Autofluorescence in age-related Macular degeneration (FAM) Study, Holz et al. used repeated FAF images to assess the progression of GA.[17] Over a median follow-up period of 1.80 years, the median ER of GA lesions was 1.52 mm^2/year. This study also reported that variable progression rates of GA appeared to depend on distinct FAF patterns around GA and these patterns may serve as prognostic indicators of disease progression. However, there are limitations to the use of this FAF strategy such as the assumption that the absence of autofluorescence truly represents loss of RPE,

photoreceptors, and choriocapillaris; the increased difficulty of detecting GA and its boundaries in the presence of cataracts; and the difficulty in identifying the boundaries of GA in the proximity of the central macula due to the retinal xanthophylls which absorb the excitation light and block FAF from the underlying RPE when using SLO imaging system.

Spectral domain optical coherence tomography (SDOCT) offers a third option for imaging GA. SDOCT, also known as fourier domain OCT, compiles a collection of B-scans into a three dimensional data set which can be used to create an OCT fundus image (OFI) by summing the signal of each of the A-scans and viewing their relative values *en face*.[18-20] This *en face* OFI permits visualization of GA as a bright area on the image due to the increased penetration of light into the choroid where atrophy has occurred in the macula. The increased OCT signal associated with GA arises from the absence of the RPE and choriocapillaris which are the two layers of the eye that normally cause the incident light to scatter thus preventing deeper transmission of light into the choroid. The brightness on the OFI results from the summation of this increased light penetration relative to the surrounding tissue which still has the intact RPE and choriocapillaris. [20-24] Lujan et al. previously reported that SDOCT fundus images can be used to identify and quantitate areas of GA.[25] The OFI appeared to correlate well with the GA appreciated on clinical examination, fundus photography, and autofluorescence imaging.

This current study examines the reproducibility of measuring the area of GA from the OFI and assesses the ER of GA based on the OFI with the goal of identifying eyes best suited for enrollment into clinical trials designed to explore new treatments which could slow or stop the progression of GA in AMD.

Subjects and Methods

Subjects

Patients were recruited from an outpatient clinic at the Bascom Palmer Eye institute. Approval for the collection and analysis of SDOCT images was obtained from the Institutional Review Board at the University of Miami Miller School of Medicine and all patients signed research informed consent. The study was performed in accordance with Health Insurance Portability and Accountability Act of 1996 (HIPAA) regulations.

Patients enrolled in the study were older than 50 years of age with the diagnosis of advanced atrophic AMD in at least one eye. The GA could be unifocal or multifocal and eyes with at least two examinations and a minimum follow-up of at least 6 months were analyzed in this study. Patients were excluded from the study if the study eye demonstrated areas of peripapillary atrophy communicating with the area of macular GA. Patients were also excluded if the GA extended outside the central scanning area which was a square centered on the fovea with dimensions 6mm × 6mm. Additional exclusion criteria for the study eye included evidence of neovascular AMD, a history of retinal surgery (including laser treatment), any sign of diabetic retinopathy, a history of retinal vascular occlusion, and a history or evidence of an inherited retinal degeneration. The major efficacy endpoints were the reproducibility of the areas measured on the OFI and the enlargement rates of GA.

OCT Fundus Image

SDOCT images were obtained using the Cirrus HD-OCT (Carl Zeiss Meditec, Inc., Dublin, CA). This SDOCT device has an axial resolution of 5μm and has a scanning rate of 27,000 A-scans per second. The central macula of each study eye was imaged using a 200×200 raster scan pattern. The first number in the 200×200 pattern refers to the number of A scans used to form each horizontal B- scan, whereas the second number is the total number of horizontal B-scans. The SDOCT was calibrated so that the horizontal and vertical

dimensions of the OFI generated from all 40000 A-scans measured 6mm × 6mm on the retina. The total scan time was 1.48 seconds. All scans were performed by a single research technician. All scans were performed between 01/01/07 and 06/01/09, using a single Cirrus Spectral Domain OCT instrument and performed after dilation of the pupil with one drop of 2.5% phenylephrine hydrochloride and 1% tropicamide. Attempts were made to perform at least 5 scans on each patient; however low-quality scans with signal strength less than 7 and scans with motion artifacts were discarded in the analysis.

The SDOCT *en face* fundus image (OFI) was obtained for each three-dimensional data set by summing all pixel intensity values along individual A-scans as provided by the commercially available image processing software. These OFIs were then used to measure the area of GA and calculate the ER.

Quantitation of GA

The OFI for each patient was exported as a .bmp file measuring 200 pixels by 200 pixels which represented an area of 6mm × 6mm on the retina. Each pixel corresponded to 30 microns which is the limit of our lateral resolution while the limit of the axial resolution is 5 microns. The area of GA was quantified by using a CintiQ WACOM digitizing tablet with its special pencil (WACOM Corp., Vancouver, WA) and image analysis software (Adobe Photoshop CS2; Adobe Systems Inc, San Jose, California, USA). Two graders (ZY and MF) outlined the areas of GA identified on the OFI. In cases where there were spared areas within a larger area of GA, these spared areas were subtracted from the total area of GA measured using the outer boundary. In the cases in which the limits of geographic atrophies were ambiguous, both graders discussed and reached an agreement on the areas to be included before drawing the final outline. The encircled area was then quantified using software written as a MATLAB (R2006a) routine which converted the number of pixels into the area of GA. The pixel area was converted to square millimeters using the same fixed ratio established by the calibrated SDOCT (the conversion factor per pixel was 0.0009 or $36mm^2/40000$ pixels). On follow-up, for each sequential pair of images, the difference in areas was calculated and the enlargement rate was determined. GA was classified into two possible configurations, either unifocal or multifocal, based on the number of atrophic areas present on the OFI.

Statistical Methods

Scans were performed on the eyes of patients with GA and the reproducibility of GA measurements was assessed. Each scan was reviewed for quality, and scans with signal strength less than 7 as well as scans with motion artifacts were categorized as low-quality scans and were discarded. Test-retest standard deviations of GA area measurements were calculated for each eye. Since test-retest standard deviations of area measurements were correlated with lesion size and lesion size was expressed as an area measurement, the reproducibility analyses were conducted on the data following a square-root transformation. The intraclass correlation coefficient of reproducibility was used as a summary statistic to quantify the test-retest reproducibility of repeat scans collected on the same day.[26] A separate analysis was performed to assess inter-grader agreement of area measurements made from each image. In addition to intraclass correlation coefficient calculations, Bland-Altman plots were constructed to determine limits of agreement between the two graders and check if the differences between grading were similar over the range of area measurements.[27]

Enlargement rate (ER) was calculated based on two visits (baseline visit and last follow up visit). The change in lesion size between these two visits (last follow up and baseline) was divided by the time of follow up (in years). ER was calculated for lesion size both on the

original area scale and after transforming the measurements to the square-root scale. Statistical analysis of baseline factors associated with the ER included a calculation of the Pearson correlation coefficient. This Pearson correlation coefficient was used to assess the strength of the correlation between ER, baseline area, and follow-up time. In an additional analysis, measurements of lesion growth, prior to normalization as a rate, were divided into groups based on three-month intervals of follow-up time. These groups were used to study the correlation between standard deviation of lesion growth and mean lesion growth. Linear regression was used to model the relationship between the standard deviation of measured growth and the mean of measured growth. Since all lesions grew, the regression line for mean growth of zero was forced through the test-retest standard deviation estimate. All statistical calculations were carried out with the software SPSS V17.0 (SPSS Inc. Chicago, IL, USA). Statistical significance was defined as $p < 0.05$.

Results

Of the 338 patients with GA scanned using the SDOCT protocol, 86 eyes of 64 patients (37 women; 58%) met the inclusion criteria and were analyzed. Median age at first examination was 83 years with a range of 63 to 94 years. Overall, median follow-up for all eyes was 1.11 years (range: 0.5 to 2.2 years). Bilateral GA was present in 39% (25 patients). Twenty three eyes (26%) were classified with a single area of GA while 63 eyes (73%) were classified as having multifocal lesions. The mean total area at baseline was 4.59 mm^2 (1.8 DA) with a median total area of 3.15 mm^2 (1.24 DA) with a range from 0.12 to 16.635 mm^2.

Test-retest reproducibility of measurements by a single grader

To assess the reproducibility of GA measurements, a total of 188 scans were collected from one eye of 42 patients, 3 to 7 scans per eye. Thirty-two eyes had at least 3 or more good quality scans encompassing the entire area of GA with good signal strength and without any movement artifacts. While only one good quality scan was needed to perform an area measurement, a minimum of 3 good quality scans were deemed necessary to assess the reproducibility of the area measurements. For this reason, the 32 eyes with at least 3 good quality scans were used to assess the reproducibility of the area measurements and these scans were included in the reproducibility analysis (127 scans (68%) out of the total 188 scans). Figure 1A demonstrates the reproducibility of these measurements and it can be appreciated that larger lesions are associated with correspondingly larger test-retest standard deviations. The correlation between lesion size and test-retest standard deviations was statistically significant (Figure 1A; $r=0.60$, $p<0.001$; Spearman $r=0.73$, $p<0.001$ $n=32$). This is a consequence of measuring areas (as opposed to linear distances) and is not unexpected. When a square-root transformation of the lesion area measurements is performed prior to the calculation of test-retest standard deviations, the correlation between lesion size and test-retest standard deviations is no longer apparent (Figure 1B; $r=0.07$, $p=0.72$; Spearman $r=0.12$, $p=0.51$ (ns), $n=32$). Reproducibility, as assessed with the intraclass correlation coefficient, was excellent on both the original area scale (ICC = 0.995) and on the square-root scale (ICC=0.996).

Use of the square-root transformed data allows the inclusion of all lesion sizes in the calculation of an estimated single pooled test-retest standard deviation which was found to be 0.030 mm. This standard deviation applies only to measurements on the square-root scale. It cannot be squared to obtain the standard deviation of the original area measurements. Therefore, a detectable change in the square-root size of GA is $\sqrt{2} \times 1.96 \times 0.030 = 0.083$ mm.[28] Thus, a true change from the original area measurement that isn't likely to be due to the test-retest variability can be obtained from the following equation: $[(\text{baseline area})^{05} + 0.083]^2 - \text{baseline area}$. For example, a change beyond test-retest variability for a lesion with baseline size of 1 DA (2.54 mm^2) would be an increase to 1.1 DA (2.8mm^2) or a

10% increase. Similarly, detectable changes for lesions with baseline sizes of 0.5 DA (1.27 mm^2), 2.0 DA (5.1 mm^2), and 3.0 DA (7.62 mm^2), would be an increase to 0.58 DA (15% increase), 2.15 DA (7.5% increase) and 3.18 DA (6% increase), respectively. For an individual lesion, any increase in total lesion area smaller than this predicted minimal change could be solely due to the test-retest variability.

Inter-grader Agreement

The intraclass correlation coefficients, a measure of agreement between two graders, were 0.999 and 0.997 for the baseline lesion areas and the last visit areas, respectively. Bland-Altman graphs relate the difference between graders and the average of the two grading (Figures 2A, 2B, available at http://aaojournal.org). Overall, there was little difference between measurements made by the two graders. When plotted on the original area scale (Figure 2A, available at http://aaojournal.org), inter-grader differences were smaller for small lesions, especially those less than $4mm^2$. However, when plotted on the square-root scale, inter-grader differences were uniform across the range of lesion sizes (Figure 2B, available at http://aaojournal.org). On the square root scale, inter-grader differences at baseline and follow-up averaged -0.4mm at baseline and -0.2mm at follow-up. There was no correlation between the differences and the lesion sizes (r^2=0.008 and 0.002 at baseline and follow-up, respectively).

Enlargement Rate (ER)

Lesions from 86 eyes of 64 patients were followed for intervals ranging from 6 months to 2.2 years. Figures 3A and 3B display the relationship between the baseline area of GA and the ER. On the original area scale, the correlation between ER and baseline area was highly significant (Figure 3A; r=0.45, p<0.001; Spearman r=0.53, p<0.001); however, there was no correlation between ER and baseline area using the square root transformed data (Figure 3B; r=-0.09, p=0.40; Spearman r=-0.06, p=0.59). The ER, which is growth expressed as change per year, appears constant over the follow-up time for this cohort of lesions on both the original area scale (Figure 4A [available at http://aaojournal.org]; r=0.13, p=0.25; Spearman r=0.15, p =0.16) and the square root area scale (Figure 4B [available at http://aaojournal.org]; r=0.08, p=0.46; Spearman r=0.10, p=0.38). The mean ER, which depends on the distribution of baseline lesion areas in this cohort, was 1.20 mm^2/yr (standard deviation (SD): 0.88 mm^2/yr) with a median ER of 1.03 mm^2/yr and a range from 0.01 to 3.62 mm^2/yr. The mean baseline lesion size was 4.59 mm^2 (SD: 4.17 mm^2) with a median of 3.15 mm^2 and a range from 0.12 to 16.64 mm^2. The mean ER for the square root of lesion area did not correlate with either baseline size or time followed and was found to be 0.28 mm/yr (SD: 0.17 mm/yr) with a median ER of 0.26 mm/yr and a range from 0.01 to 0.82 mm/yr.

To assess the relationship between lesion growth and variability of lesion growth, lesions were divided into groups with follow-up intervals of three months. The seven resulting groups ranged in size from 9 to 24 lesions. A highly significant correlation was found between the standard deviation of the square root area measurements and the mean of the square root area measurements (r = 0.99, p<0.001, Spearman r=0.96, p=0.001). A linear regression equation was constructed to estimate the standard deviation associated with a given level of average growth, on the square root scale, for use in calculating estimations of sample sizes for future clinical studies. The zero-growth intercept of this equation is the same as the test-retest variability of a size measurement; therefore, the regression equation was forced though the test-retest standard deviation estimate of 0.030mm at a value of zero growth. The slope of this equation was 0.509 mm.

Table 1 (available at http://aaojournal.org) provides sample size requirements for controlled clinical trials designed to evaluate potential treatments with a range of hypothetical efficacies over various follow-up periods. A treatment with high efficacy (75-100% reduction in ER compared with control) could be conducted with relatively few subjects and a treatment effect could be established in as little as 6 months. Less effective treatments would require either larger study sample sizes or longer periods of follow-up. None of the scenarios evaluated in Table 1 (available at http://aaojournal.org) suggest much advantage in extending follow-up beyond 18 months in the determination of treatment efficacy; however, this assumes that effectiveness of a treatment persists over time, which may or may not be the case for any particular treatment.

To address the question of whether a unifocal area of GA has an ER different than a multifocal lesion, we analyzed the total progression of GA based on whether there was a single area of GA (Figure 5, available at http://aaojournal.org) or multiple areas of GA at baseline (Figure 6). Of the 86 eyes, 63 (73%) were multifocal and 23 (27%) were unifocal. The mean lesion area measurement at baseline for the multifocal lesions was 3.80 mm^2 (SD=3.41) which was smaller (p=0.018) than unifocal lesions with 6.75 mm^2 (SD= 5.25). The same was true on the square root scale (p=0.020), where the mean multifocal lesion measurement at baseline was 1.77 mm (SD=0.83) compared with the mean unifocal lesion measurement at baseline of 2.31 mm (SD=1.21). There was no significant difference in the ER on the area scale between the lesions types (multifocal: mean ER = 1.25 mm^2/year (SD=0.86); Unifocal: mean ER = 1.05 mm^2/year (SD=0.93); t-test p-value=0.34). However, when the ERs for the square root of the lesion areas were analyzed, the difference was highly significant (t-test p-value =0.002) with multifocal lesions having a mean ER of 0.32 (SD=0.17) mm/year compared with unifocal lesions having a mean ER of 0.19 (0.12) mm/year. Comparison of medians gave similar results. Median ERs for area measurements were not significantly different between lesion types with multifocal lesions having a median ER of 1.05 mm^2/year and unifocal lesions having a median ER of 0.82 mm^2/year (Mann-Whitney p-value=0.19). However the difference was highly significant for the ER of the transformed data (Mann-Whitney p-value =0.001) with multifocal lesions having a median ER of 0.30mm/year compared with unifocal lesions having a median ER of 0.15mm/year. Examples of unifocal and multifocal GA imaged using SDOCT over time are shown in Figures 5 (available at http://aaojournal.org) and 6.

Discussion

This study confirms that SDOCT fundus images can be used to reproducibly quantitate areas of GA. The protocol used in this study to assess progression of GA resulted in remarkably reproducible measurements with an intraclass correlation coefficient greater than 0.99, and any value greater than 0.75 is usually considered to represent an excellent outcome.[29] This study confirmed previous observations showing that the ER of GA depends on the lesion size with larger lesions growing faster[10, 11, 17]; however, when areas were analyzed after applying a square root transformation, the enlargement rate did not show any dependence on the baseline lesion size.

For an intuitive interpretation of the square root transformation one may consider, for simplicity, a circular region of GA. The assumption that the radius (r) of the region is increasing at a constant rate would be a reasonable scenario if the lesion grows around its boundary. Simple algebra demonstrates that if the circle's radius increases at a constant rate, the rate of change for the lesion area is proportional to the baseline radius since the area measurements (πr^2) are exponentially related to the radius measurements. This would explain why the areas of larger lesions grow faster than the areas of smaller lesions even though the radius is growing at a constant rate. Under our hypothesis, the rate of change for

the square root of the lesion area would instead be constant. This same argument applies as well to the test-retest differences and inter-grader differences. It could also explain some of the difference in the growth rates of unifocal and multifocal lesions, but testing of this hypothesis requires further data collection. Our empirical findings support some utility of this simple model of lesion growth. Our results using the square root transformation of the lesion area demonstrate that, if the correct framework is used to assess lesion growth and the technology used for the measurements has sufficient precision to measure small lesions reliably, then the baseline lesion size does not have to be taken into account as an inclusion criterion for a clinical study designed to test the effect of a treatment on the change in GA over a defined follow-up period. In this study, we find that the Cirrus OCT had sufficient precision to reliably measure lesions as small as 0.12 mm^2 (0.05 DA).

The mean enlargement rate for all eyes in this study was 1.2 mm^2/year and the median enlargement rate was 1.02 mm^2/year. These growth rates are slower than the ones previously published.[3, 9-11, 17] The differences in the growth rates from previous studies may be partially attributed to the fact that our study population had a smaller baseline area with a median area of 3.15 mm^2 and a mean area of 4.59 mm^2. Overall, our lesions were probably smaller since we limited our analysis to lesions that were contained within the central 6mm × 6mm scanning area of the macula and we excluded areas that were contiguous with peripapillary atrophy. In addition to the smaller overall size of GA in our population, the slower enlargement rate in our series may be related to the use of SDOCT to measure GA or a difference in environmental and genetic risk factors in our population.[31-35] It would be interesting to look at the square root transformation of the previously published data to determine if the differences in enlargement rates between the studies could be explained by this difference in baseline lesion area measurements or in the populations.

In this study, a statistically significant correlation was found between the ER on the original area (mm^2) scale and the baseline area. This finding agrees with other published papers which reported a similar relationship between growth rate and baseline area of GA.[10,11]. In contrast to these reports, Holz et al. found that eyes with baseline total atrophy less than 2.54 mm^2 (<1 DA) (median, 1.27 mm^2; range, 0.13 to 2.47 mm^2) exhibited a significant difference in progression of atrophy compared with other groups ($P < .0001$), but for those eyes with an area of GA greater than 1 DA, there were no significant differences in progression rates when the following groups were compared: 1 to 3 DA (2.54 to 7.61 mm^2), 3 to 5 DA (7.62 to 12.69 mm^2), and 5 to 10 DA (12.70 to 25.39 mm^2). They concluded that the fundus autofluorescence pattern was more strongly correlated with the growth of GA even for small lesions (<1DA).17 Dreyhaupt et al. also found that enlargement of GA based on fundus autofluorescence measurements was not dependent on baseline atrophy,30 and Klein et al. also found that enlargement of GA based on color fundus photography measurements was not dependent on baseline atrophy over 5 years of follow up.9 Regardless of whether the enlargement rate correlates with baseline area, all the studies did show that a wide variation in ER was apparent for a given baseline area of GA. By using a square root transformation of the areas at baseline and at follow-up, our data give every indication that there is no dependence of the ER on the baseline lesion area. The wide range in the ER on the square root (mm) scale suggests that the identification of risk factors for rate of growth, other than baseline area, is an important research topic.

When analyzing the ER in different subgroups using lesion area measurements, we found there was no statistical difference between unifocal and multifocal lesions. However, when the square root transformation of the lesion area measurements at baseline and at follow-up was performed, we found a statistically significant difference between the average ER of the unifocal lesions compared with the multifocal lesions. This result is in accordance with the report by Klein et al. in which they showed that multifocal lesions grew faster than unifocal

lesions in the Beaver Dam Study.[9] One explanation for why our initial analysis using area measurements failed to identify a difference in growth rates between unifocal and multifocal lesions may have to do with the difference in mean baseline area when the unifocal lesions were compared to the multifocal lesions. On average, the unifocal lesions were larger (6.75 mm^2) than the multifocal lesions (3.79 mm^2), and if the ER is dependent on the baseline lesion area measurement, then the larger unifocal lesions would appear to be growing faster than the smaller multifocal lesions and the difference in ER between the two lesion types would be obscured by the difference in the baseline lesion area measurements. However, by taking the square transformation of the lesion area measurements, it would appear that the dependence on baseline lesion area was eliminated and the difference in ER between the two lesion types was revealed. Thus, the square root transformation of the lesion area measurements appears to eliminate the confounding variable of baseline lesion size from this analysis and should eliminate the need for stratifying lesions based on baseline lesion size in clinical studies. These results suggest the need for future studies to investigate the difference in growth rates between these lesion types and raise the question of whether future clinical trials should stratify unifocal and multifocal lesions at the time of enrollment.

In our study, the median follow-up time for all study eyes was 1.24 years (range, 0.5 to 2.2 years). Study eyes with follow-up less than a year were included because one objective of this study was to determine the minimal lesion size that could be enrolled for a study with 6 months duration. Moreover, longer average follow-up would not have been possible because SDOCT imaging has only been available recently. In contrast, Sunness et al. based their report on a median follow up time of 3 and 4.3 years respectively,[3,] 10 the AREDS series had a follow-up of 4 years11, and the Klein series was reported to be 5 years.9 It is reassuring to report that even though our average follow-up was only 1.24 years, Sunness et al. reported that the 1-year ER mirrored the findings of the 2-year ER.[10]

The measurements obtained from the OFI were highly reproducible and there was excellent agreement between graders with intraclass correlations >0.995. This means that less than one half percent of the variability in the measurements was due to differences between graders. Other studies have evaluated the reproducibility GA measurements using either color fundus photographs or fundus autofluorescence images, and the reproducibility reported using the SDOCT fundus image appears to be at least as good as or better than these other modalities.[11, 13, 16, 36] In the future, this measurement technique will be applied to larger areas of GA that extend beyond the borders of the 6mm × 6mm scanned area. Algorithms have already been developed that are capable of assembling multiple overlapping SDOCT fundus images into a larger montage of the macula so that any area of GA can be imaged and measured using this SDOCT approach.

Studies comparing the SDOCT fundus image, fundus autofluorescence, color fundus photography, and fluorescein angiography are currently underway to determine whether one approach is more useful than another in clinical practice and in clinical trials. This current study has shown that GA can be reproducibly identified, quantified, and followed using the en-face SDOCT fundus image. This study also demonstrated that the choice of a suitable measurement scale, in this case the square root of the area, may substantially simplify the design and analysis of treatment trials for GA regardless of the imaging strategy used in the study. However, the advantages of using the SDOCT fundus image include the convenience and assurance of using only one type of scan for documenting both *en face* and cross sectional images of the macula. In addition, this imaging approach for GA most likely represents the area corresponding to the loss of photoreceptors and retinal pigment epithelium which correlates with the loss of visual function.

Acknowledgments

Research supported by a grant from Carl Zeiss Meditec, Inc., Dublin, CA, an unrestricted grant from Research to Prevent Blindness. Inc., a NEI core center grant P30 EY014801 to the University of Miami, the H.A. & Mary K. Chapman Charitable Trust, Florman Family Foundation, Inc., Jerome A. Yavitz Charitable Foundation, Carl and Lily Pforzheimer Foundation, Inc., Emma Clyde Hodge Memorial Foundation and the Gemcon Family Foundation. Zohar Yehoshua is a Recipient of a Fellowship Grant from the American Physicians Fellowship for Medicine in Israel. Manuel Falcão received a Fulbright Scholarship and Portuguese Society of Ophthalmology Scholarship.

References

1. Schatz H, McDonald HR. Atrophic macular degeneration: rate of spread of geographic atrophy and visual loss. Ophthalmology. 1989; 96:1541–51. [PubMed: 2587050]
2. Potter JW, Thallemer JM. Geographic atrophy of the retinal pigment epithelium: diagnosis and vision rehabilitation. J Am Optom Assoc. 1981; 52:503–8. [PubMed: 7264141]
3. Sunness JS, Gonzalez-Baron J, Applegate CA, et al. Enlargement of atrophy and visual acuity loss in the geographic atrophy form of age-related macular degeneration. Ophthalmology. 1999; 106:1768–79. [PubMed: 10485549]
4. Maguire P, Vine AK. Geographic atrophy of the retinal pigment epithelium. Am J Ophthalmol. 1986; 102:621–5. [PubMed: 3777083]
5. Sarks JP, Sarks SH, Killingsworth MC. Evolution of geographic atrophy of the retinal pigment epithelium. Eye (Lond). 1988; 2:552–77. [PubMed: 2476333]
6. Klein R, Klein BE, Franke T. The relationship of cardiovascular disease and its risk factors to age-related maculopathy: the Beaver Dam Eye Study. Ophthalmology. 1993; 100:406–14. [PubMed: 8460013]
7. Vingerling JR, Dielemans I, Hofman A, et al. The prevalence of age-related maculopathy in the Rotterdam Study. Ophthalmology. 1995; 102:205–10. [PubMed: 7862408]
8. Hirvela H, Luukinen H, Laara E, Laatikainen L. Risk factors of age-related maculopathy in a population 70 years of age or older. Ophthalmology. 1996; 103:871–7. [PubMed: 8643241]
9. Klein R, Meuer SM, Knudtson MD, Klein BE. The epidemiology of progression of pure geographic atrophy: the Beaver Dam Eye Study. Am J Ophthalmol. 2008; 146:692–9. [PubMed: 18672224]
10. Sunness JS, Margalit E, Srikumaran D, et al. The long-term natural history of geographic atrophy from age-related macular degeneration: enlargement of atrophy and implications for interventional clinical trials. Ophthalmology. 2007; 114:271–7. [PubMed: 17270676]
11. AREDS Research Group. Change in area of geographic atrophy in the Age-Related Eye Disease Study: AREDS report number 26. Arch Ophthalmol. 2009; 127:1168–74. [PubMed: 19752426]
12. Sunness JS, Ziegler MD, Applegate CA. Issues in quantifying atrophic macular disease using retinal autofluorescence. Retina. 2006; 26:666–72. [PubMed: 16829810]
13. Scholl HP, Peto T, Dandekar S, et al. Inter- and intra-observer variability in grading lesions of age-related maculopathy and macular degeneration. Graefes Arch Clin Exp Ophthalmol. 2003; 241:39–47. [PubMed: 12545291]
14. Pirbhai A, Sheidow T, Hooper P. Prospective evaluation of digital non-stereo color fundus photography as a screening tool in age-related macular degeneration. Am J Ophthalmol. 2005; 139:455–61. [PubMed: 15767053]
15. Age-Related Eye Disease Study Research Group. The Age-Related Eye Disease Study severity scale for age-related macular degeneration: AREDS report no. 17. Arch Ophthalmol. 2005; 123:1484–98. [PubMed: 16286610]
16. Sunness JS, Bressler NM, Tian Y, et al. Measuring geographic atrophy in advanced age-related macular degeneration. Invest Ophthalmol Vis Sci. 1999; 40:1761–9. [PubMed: 10393046]
17. Holz FG, Bindewald-Wittich A, Fleckenstein M, et al. FAM-Study Group. Progression of geographic atrophy and impact of fundus autofluorescence patterns in age-related macular degeneration. Am J Ophthalmol. 2007; 143:463–72. [PubMed: 17239336]
18. Jiao, S.; Knighton, RW.; Huang, X., et al. Simultaneous acquisition of sectional and fundus ophthalmic images with spectral-domain optical coherence tomography; Opt Express [serial

online]. 2005 [June 19, 2010]. p. 444-52.Available at: http://www.opticsinfobase.org/abstract.cfm?URI=oe-13-2-444

19. Wojtkowski M, Srinivasan V, Fujimoto JG, et al. Three-dimensional retinal imaging with high-speed ultrahigh-resolution optical coherence tomography. Ophthalmology. 2005; 112:1734–46. [PubMed: 16140383]
20. Bearelly S, Chau FY, Koreishi A, et al. Spectral domain optical coherence tomography imaging of geographic atrophy margins. Ophthalmology. 2009; 116:1762–9. [PubMed: 19643488]
21. Srinivasan VJ, Monson BK, Wojtkowski M, et al. Characterization of outer retinal morphology with high-speed, ultrahigh-resolution optical coherence tomography. Invest Ophthalmol Vis Sci. 2008; 49:1571–9. [PubMed: 18385077]
22. Drexler W, Fujimoto JG. State-of-the-art retinal optical coherence tomography. Prog Retin Eye Res. 2008; 27:45–88. [PubMed: 18036865]
23. Yasuno, Y.; Hong, Y.; Makita, S., et al. In vivo high-contrast imaging of deep posterior eye by 1-microm swept source optical coherence tomography and scattering optical coherence angiography; Opt Express [serial online]. 2007 [June 19, 2010]. p. 6121-39.Available at: http://www.opticsinfobase.org/abstract.cfm?URI=oe-15-10-6121
24. Hammer M, Roggan A, Schweitzer D, Muller G. Optical properties of ocular fundus tissues--an in vitro study using the double-integrating-sphere technique and inverse Monte Carlo simulation. Phys Med Biol. 1995; 40:963–78. [PubMed: 7659735]
25. Lujan BJ, Rosenfeld PJ, Gregori G, et al. Spectral domain optical coherence tomographic imaging of geographic atrophy. Ophthalmic Surg Lasers Imaging. 2008; 39(suppl):S8–14.
26. Fleiss, JL. The Design and Analysis of Clinical Experiments. New York: Wiley; 1986. p. 1-28.
27. Bland JM, Altman DG. Statistical methods for assessing agreement between two methods of clinical measurement. Lancet. 1986; 1:307–10. [PubMed: 2868172]
28. Budenz DL, Fredette MJ, Feuer WJ, Anderson DR. Reproducibility of peripapillary retinal nerve fiber thickness measurements with Stratus OCT in glaucomatous eyes. Ophthalmology. 2008; 115:661–6. [PubMed: 17706287]
29. Fleiss, J. Statistical Methods for Rates and Proportions. 2nd. New York: Wiley; 1981. p. 218
30. Dreyhaupt J, Mansmann U, Pritsch M, et al. Modelling the natural history of geographic atrophy in patients with age-related macular degeneration. Ophthalmic Epidemiol. 2005; 12:353–62. [PubMed: 16283987]
31. Seddon JM, Francis PJ, George S, et al. Association of *CFH Y402H* and *LOC387715 A69S* with progression of age-related macular degeneration. JAMA. 2007; 297:1793–800. [PubMed: 17456821]
32. Tomany SC, Wang JJ, Van Leeuwen R, et al. Risk factors for incident age-related macular degeneration: pooled findings from 3 continents. Ophthalmology. 2004; 111:1280–7. [PubMed: 15234127]
33. Smith W, Assink J, Klein R, et al. Risk factors for age-related macular degeneration: pooled findings from three continents. Ophthalmology. 2001; 108:697–704. [PubMed: 11297486]
34. Jager RD, Mieler WF, Miller JW. Age-related macular degeneration. N Engl J Med. 2008; 358:2606–17. [PubMed: 18550876]
35. Klein R. Overview of progress in the epidemiology of age-related macular degeneration. Ophthalmic Epidemiol. 2007; 14:184–7. [PubMed: 17896295]
36. Schmitz-Valckenberg S, Fleckenstein M, Gobel AP, et al. Evaluation of autofluorescence imaging with the scanning laser ophthalmoscope and the fundus camera in age-related geographic atrophy. Am J Ophthalmol. 2008; 146:183–92. [PubMed: 18514607]

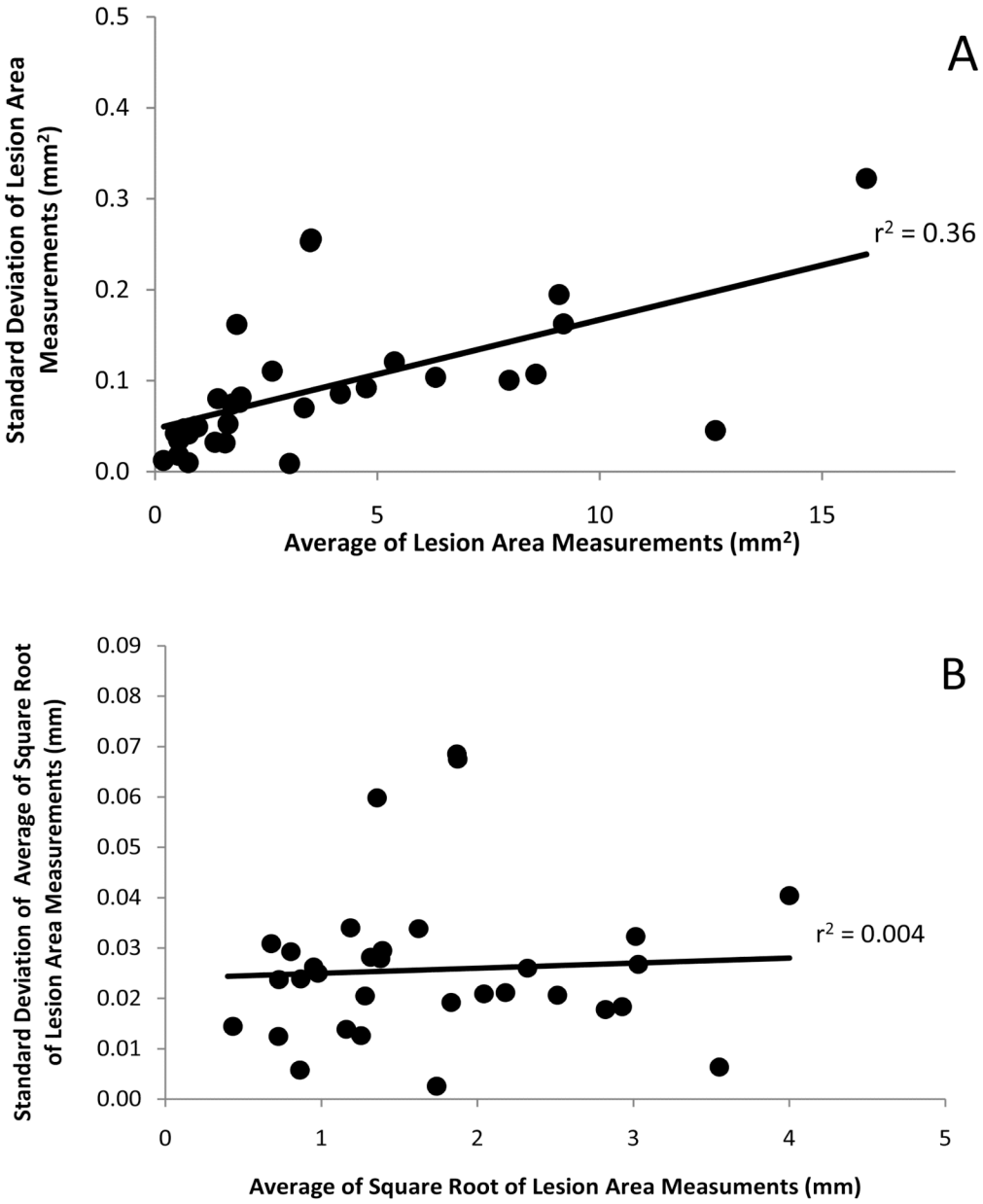

Figure 1.

Reproducibility of Lesion Size Measurements

A. Average of repeated lesion area measurements from multiple scans obtained from each eye plotted against their standard deviations.

B. Average of the square root of repeated lesion area measurements from multiple scans obtained from each eye plotted against their standard deviations.

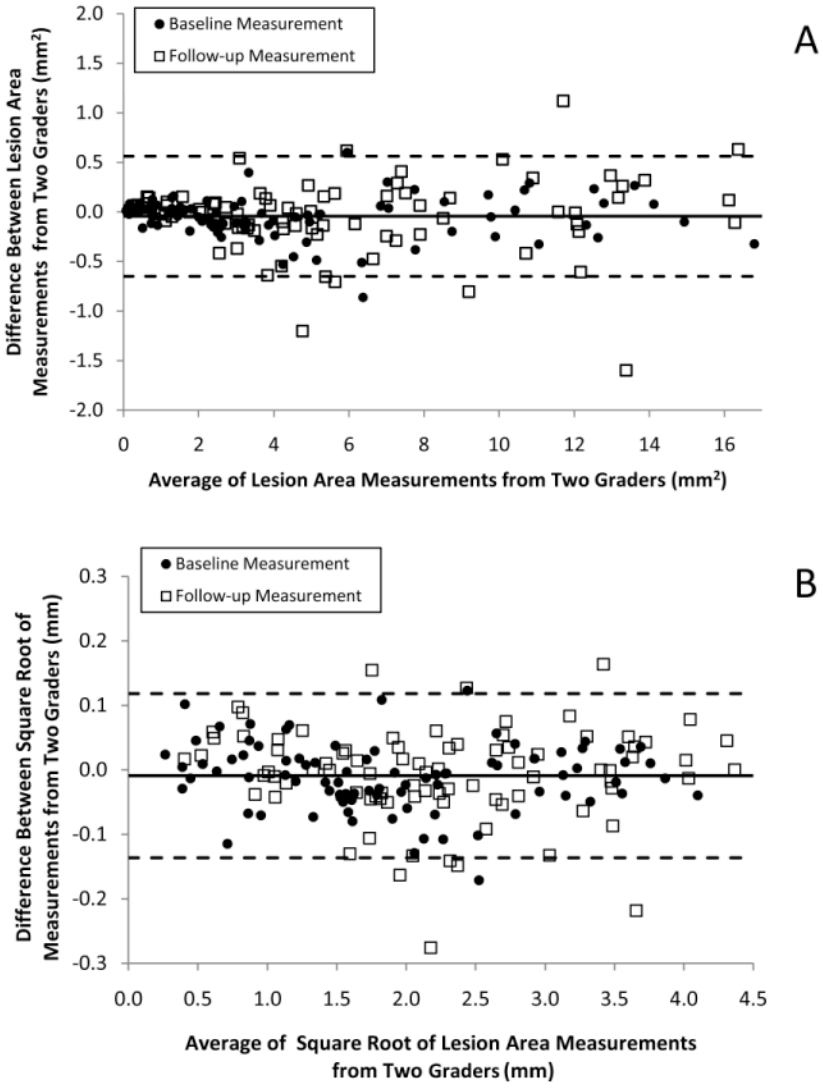

Figure 2.

Bland-Altman Plots of Lesion Size Measurements from Two Graders

A. The agreement between lesion area measurements performed by two graders at baseline and last follow-up displayed using Bland Altman plots. Solid line depicts the average difference between two graders. Dashed lines depict the Bland-Altman limits of agreement. The coefficient of variation was 7.7%.

B. The agreement between the square root of lesion area measurements performed by two graders at baseline and last follow-up displayed using Bland Altman plots. Solid line depicts the average difference between two graders. Dashed lines depict the Bland-Altman limits of agreement. The coefficient of variation was 3.2%.

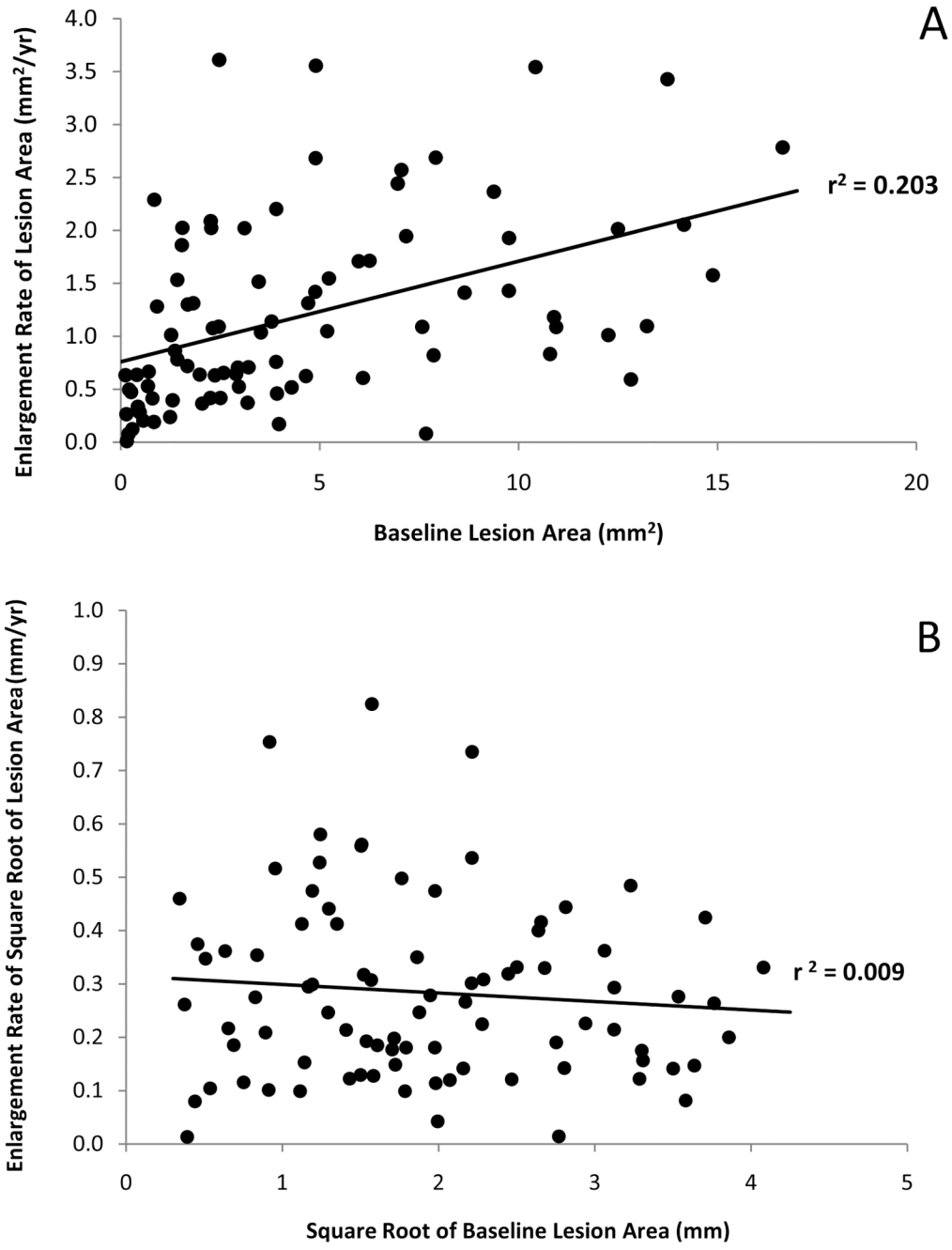

Figure 3.

Relationship between Enlargement Rate and Baseline Lesion Size

A. Scatter plot showing the enlargement rate as a function of baseline lesion area.

B. Scatter plot showing the enlargement rate based on the square root of the lesion area measurements as a function of the square root of the baseline lesion area.

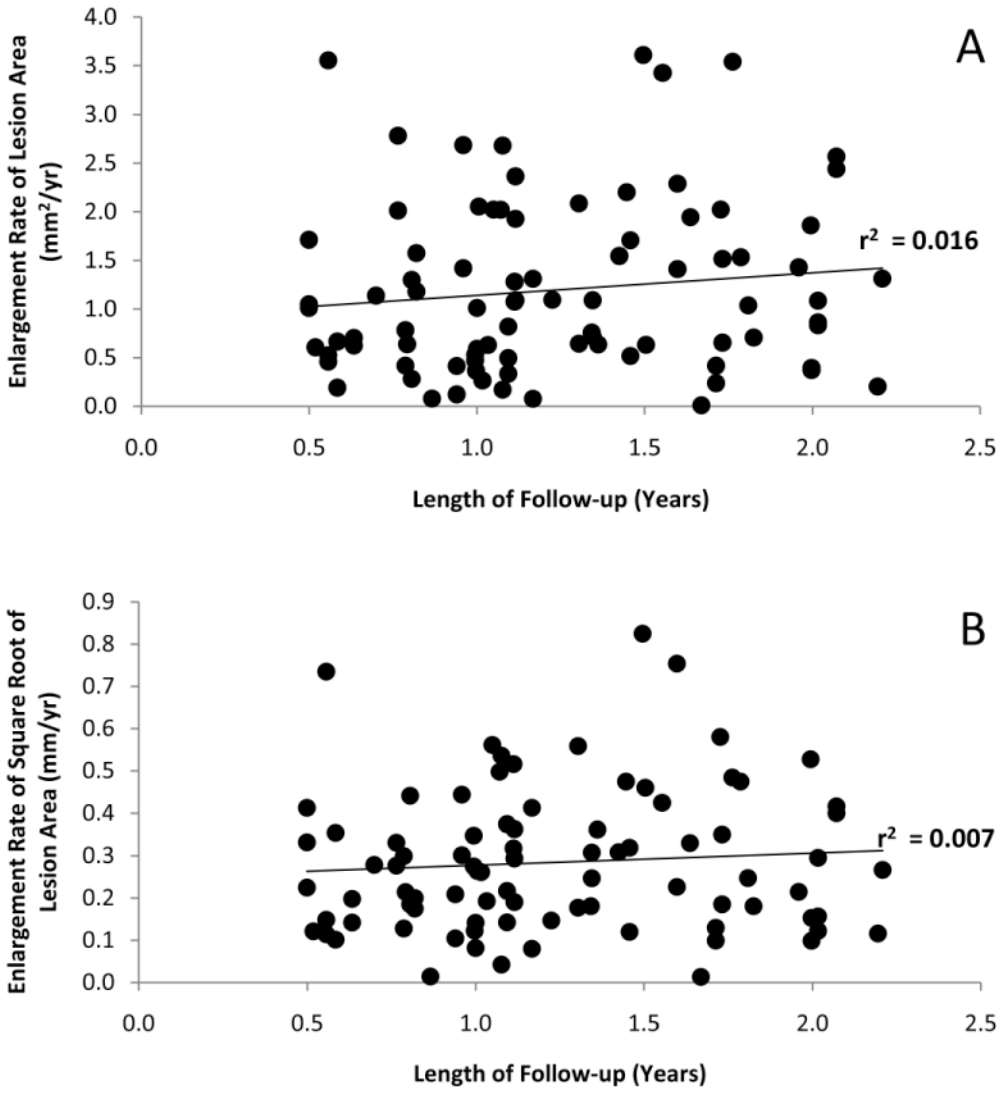

Figure 4.

Relationship between Enlargement Rate and Length of Follow-up

A. Scatter plot showing the relationship between the enlargement rate of lesion area and years of follow-up.

B. Scatter plot showing the relationship between the enlargement rate of the square root of lesion area and years of follow-up.

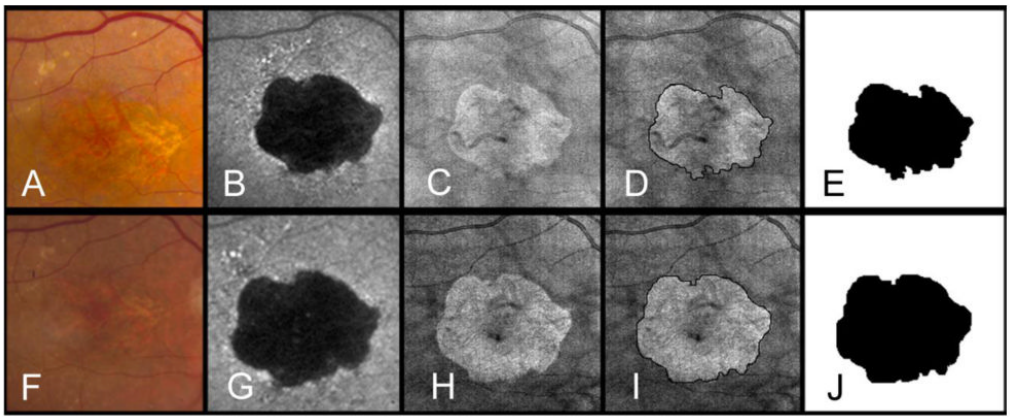

Figure 5.

Unifocal area of geographic atrophy (GA) as seen by fundus photography (A,F), fundus camera-based autofluorescence* (B,G), and OCT fundus imaging (C, H) at baseline (A-E) and at the end of a 14 month follow-up period (F-J). The boundaries of GA were manually outlined on the OCT fundus image at baseline (D) and at the end of the follow up period (I). Areas of GA were calculated as 7.6 mm^2 (E) and 10.09 mm^2 (J). Frames E and J show a clear growth in the area of GA over time. This difference was used to calculate the yearly enlargement rate (2.17 mm^2/year). On a square root scale the enlargement rate was 0.36 mm/year.

*Topcon TRC-501X color fundus camera (Topcon Medical Systems, Oakland, NJ) with filters by Spectrotech, Inc. (Saugus, MA) having an excitation bandpass filter centered at a wavelength of 580 nm and a barrier bandpass filter centered at a wavelength of 695 nm.

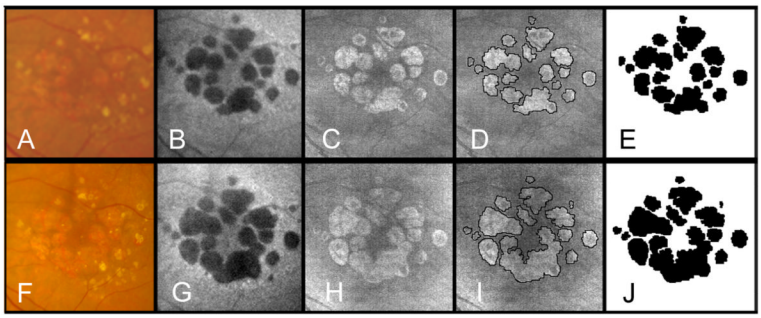

Figure 6.

Large multifocal area of geographic atrophy (GA) as seen by fundus photography (A,F), fundus camera-based autofluorescence* (B,G), and OCT fundus imaging (C,H) at baseline (A-E) and at the end of a 12 month follow-up period (F-J). The boundaries of GA were manually outlined on the OCT fundus image at baseline (D) and at the end of the follow up period (I). Areas of GA were calculated as 6.88 mm^2 (E) and 9.20mm^2 (J). Frames E and J show a clear growth in the area of GA over time. This difference was used to calculate the yearly enlargement rate (2.32 mm^2/year). On a square root scale the enlargement rate was 0.41 mm/year.

*Topcon TRC-501X color fundus camera (Topcon Medical Systems, Oakland, NJ) with filters by Spectrotech, Inc. (Saugus, MA) having an excitation bandpass filter centered at a wavelength of 580 nm and a barrier bandpass filter centered at a wavelength of 695 nm.

Table 1

Sample Size Estimates for Clinical Trials Using the Square Root of Lesion Area to Investigate Treatment Efficacy

Months Followed	No Treatment		100% reduction in Enlargement Rate with treatment*				75% reduction in Enlargement Rate with treatment*				50% reduction in Enlargement Rate with treatment*				25% reduction in Enlargement Rate with treatment*			
	Predicted change in square-root lesion area (mm)		Predicted Change in square-root lesion area (mm)		Sample Size required per group for power of		Predicted Change in square-root lesion area (mm)		Sample Size required per group for power of		Predicted Change in square-root lesion area (mm)		Sample Size required per group for power of		Predicted Change in square-root lesion area (mm)		Sample Size required per group for power of	
	Mean†	SD‡	Mean	SD‡	80%	90%	Mean	SD‡	80%	90%	Mean	SD‡	80%	90%	Mean	SD‡	80%	90%
6	0.14	0.10	0.00	0.03	5	6	0.04	0.05	10	14	0.07	0.07	24	32	0.11	0.08	144	192
12	0.28	0.17	0.00	0.03	<5	5	0.07	0.07	7	9	0.14	0.10	16	21	0.21	0.14	78	105
18	0.42	0.24	0.00	0.03	<5	<5	0.11	0.08	6	7	0.21	0.14	14	19	0.32	0.19	74	99
24	0.56	0.32	0.00	0.03	<5	<5	0.14	0.10	6	7	0.28	0.17	14	18	0.42	0.24	65	86

*The required sample sizes for a clinical trial comparing natural history growth of the square-root area (mm) to 100%, 75%, 50%, and 25% reduction in enlargement rate with treatment. Calculations assume analysis with independent samples t-test with unequal variances

†Assuming Enlargement Rate of square root lesion area of 0.28 mm/year

‡Standard deviation (SD) was estimated as a linear function of the mean growth of the square root of the lesion area; SD = (0.509)×(Mean Growth) + 0.030 (see results)

Ophthalmology. Author manuscript; available in PMC 2012 April 1.